Dalton Transactions

Accepted Manuscript

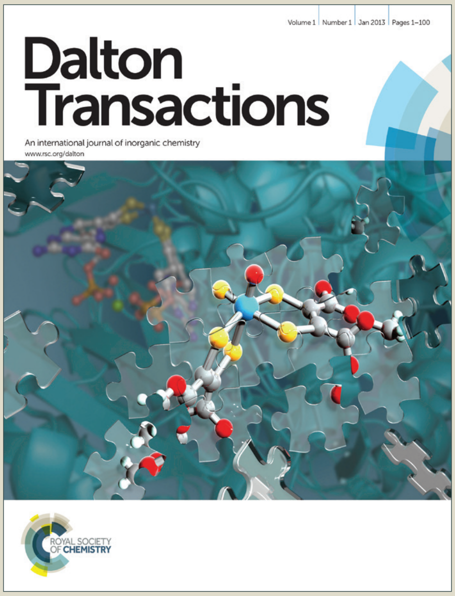

ROYAL SOCIETY OF CHEMISTRY

www.rsc.org/dalton

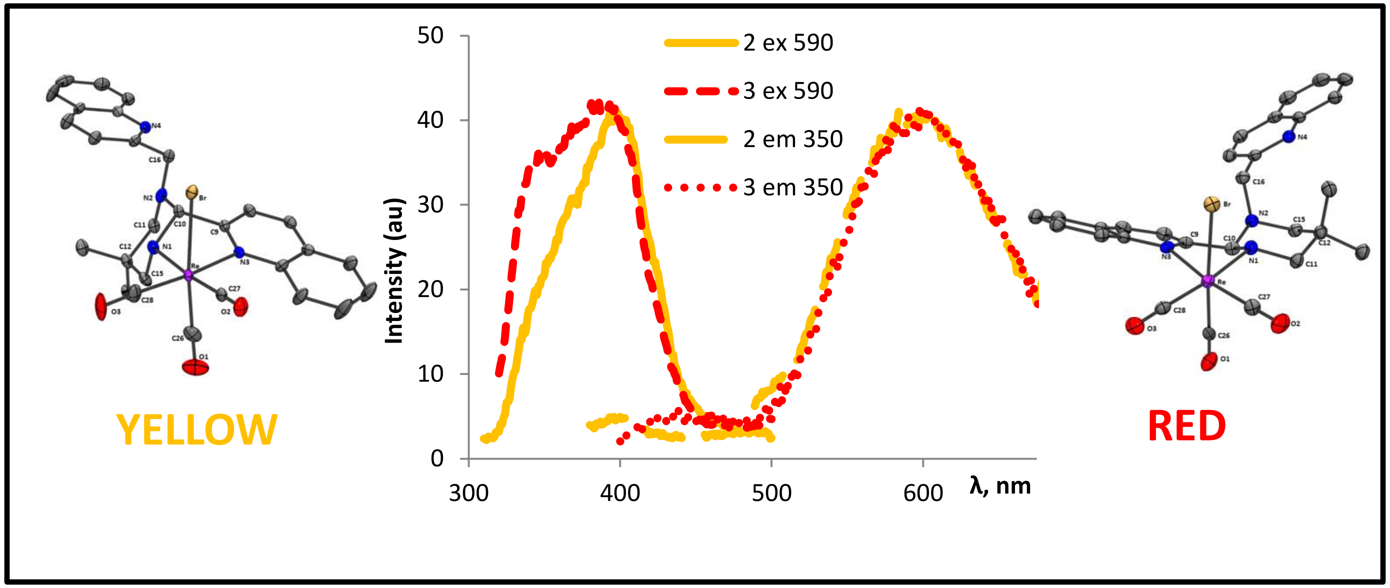
YELLOW
RED
2 ex 590
3 ex 590
2 em 350
3 em 350
Intensity (au)
λ, nm
0
10
20
30
40
50
300
400
500
600
N4
C16
N2
Br
C11
C10
C9
C12
N1
N3
C15
Re
C27
C28
O3
O2
C26
O1

Cite this: DOI: 10.1039/c0xx00000x

www.rsc.org/xxxxxx

ARTICLE TYPE

Stereoelectronic Control of Photophysics: Red and Yellow Axial and Equatorial Anomers of a Rhenium-Quinoline Complex

Rachel H. Platel,*[a] Michael P. Coogan[a] and James A. Platts[b]

Received (in XXX, XXX) Xth XXXXXXXXX 20XX, Accepted Xth XXXXXXXXX 20XX
DOI: 10.1039/b000000x

A novel quinoline-substituted pyrimidine ligand forms two different coloured complexes upon reaction with $Re(CO)_5Br$. These compounds display distinct photophysical properties that are dictated by their stereochemistry.

Rhenium bis(imine) complexes $[Re(CO)_3(N\text{^}N)L]$ often have interesting photophysical properties, usually emitting from ^{3}MLCT states with long luminescence lifetimes and large Stokes shifts.[1,2] Their absorption and emission properties have been widely investigated and are exploited in areas as diverse as biological imaging,[3] OLEDs,[4] photocatalysis[5] and photovoltaics.[6] Certain examples are responsive to the presence of other ions or molecules and have been used in luminescence sensing and assays.[7] These complexes all have a *fac*- geometry and, in the cases of symmetrical N^N ligands, are achiral, so to the best of our knowledge have not been used as stereochemical probes.

Complexes involving a Het^NR^Het motif (het = Py, quinoline or similar) such as dipicolyl amine have been applied in imaging involving bioconjugation to peptides through a lysine side-chain in the Single Amino Acid Chelate (SAAC) approach (Fig. 1).[8]

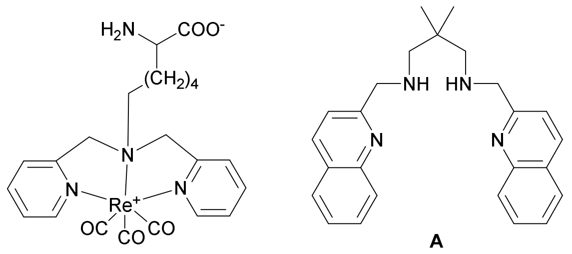

Fig. 1 Example of the SAAC approach and target ligand **A**.

These complexes show particularly rich and versatile photophysics with the dipicolyl amine complexes being UV absorbing, and visible emitting, the quinoline analogues red shifted into the visible for both transitions, and the thiazoles showing emission wavelengths which vary as a function of excitation.[9]

If the electron density in the excited state is located on one or both of the heterocycles with little or no contribution from the central NR unit, and little interaction between them, then an isolated Het^NR unit could be expected to show similar photophysics. The coordinatively unsaturated core would then allow for either further tuning of the photophysics, or interaction with ions and molecules in sensing applications. Reductive amination of heterocyclic aldehydes with diamines, gives dimeric analogues of the isolated NR^Het unit (i.e. a Het^NRN^Het motif) which could form stereochemically interesting complexes with 2 or 3 coordinated nitrogen atoms, with the possibility of fluxionality between these cases.

As a preliminary investigation into this area we attempted to prepare the tethered bis(aminoquinoline) ligand **A** (Fig. 1), which, by analogy with the SAAC analogue, we anticipated should form a $Re(CO)_3$ complex with lower energy absorption and emission than the pyridine analogues.

Reaction of 2,2-dimethyl-1,3-propane diamine with 2 eq. quinoline 2-carboxaldehyde, followed by reduction with an excess of sodium borohydride gave, upon work up, a brown solid.

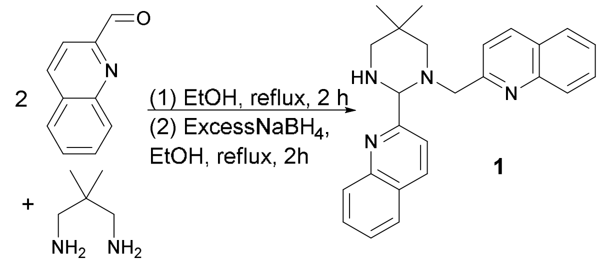

Scheme 1 Synthesis of **1**.

A ^{1}H NMR spectrum of the crude reaction mixture indicated a mixture of products was present. Recrystallization from a hot dichloromethane solution provided **1** cleanly, as a colourless, crystalline solid in 61% yield (Scheme 1). Characterization data revealed that this was not the expected bis(aminoquinoline) product, **A**, but rather, that substituted hexahydropyrimidine **1** had been formed. X-ray crystallographic analysis of a single crystal grown from a dichloromethane solution confirmed the ligand structure (Fig. 2).

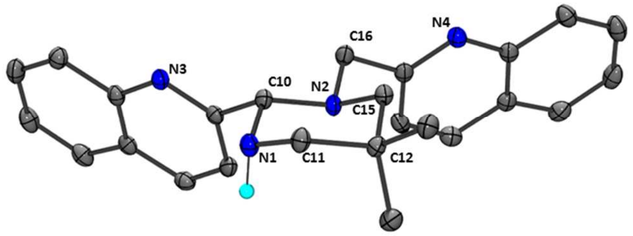

Fig. 2 Molecular Structure of **1**. Thermal ellipsoids are shown at 50% level. Non-NH hydrogens are omitted for clarity.

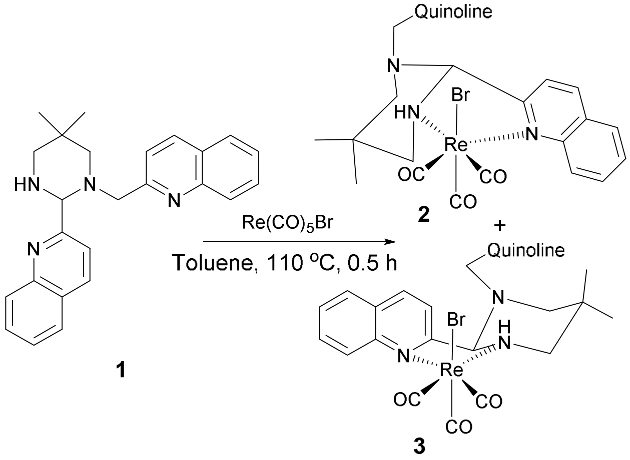

Scheme 2 Synthesis of **2** and **3**.

In the solid state structure of **1**, the pyrimidine adopts a chair conformation, with both quinoline substituents occupying equatorial positions. Non-quinoline bond lengths fall within the expected values for C–N single bonds, ranging from 1.4568(15) to 1.4868(14) Å.

The ^{1}H NMR spectrum of compound **1** suggests that this structure is maintained in solution (dynamic equilibrium is assumed, but with a vanishingly small concentration of the ring-open form). In particular, eleven aromatic signals indicate inequivalence of the quinoline moieties, a singlet at 4.49 ppm is assigned to the methine H and a 4-bond W coupling is observed between equatorial hydrogens on C11 and C16, with $^4J_{HH}$ of 1.6 Hz. The ligand exists as a single anomer with both quinoline groups equatorial in order to reduce the energetically disfavoured axial interactions between hydrogens and the bulky quinoline groups. We propose that **1** is formed after reduction of one of the imine groups. Nucleophilic attack by the secondary amine at the imine carbon followed by proton transfer gives the pyrimidine, **1**. The 2,2-dimethyl substituents on the diamine fragment favour cyclization through this reactivity through the Thorpe-Ingold effect.[10] Indeed, use of unsubstituted 1,3-diaminopropane as the amine in this reaction provides a ligand analogous to **A** in high yield.

The reaction between **1** and an equimolar amount of Re(CO)$_5$Br was carried out in toluene solution at 100 °C (Scheme 2). After 30 min a pale yellow precipitate had formed. This was filtered off to leave a red solution, from which red crystalline material deposited over the course of 48 h at room temperature. ^{1}H NMR spectroscopy indicated that the yellow powder and red crystals were different species, but could both be isolated cleanly from the reaction mixture with a minimal number of manipulations.

Single crystals were grown of both the yellow powder product, **2**, and the red product, **3**, from saturated solutions of acetonitrile/toluene and toluene respectively and analysed by X-ray crystallography (Figs. 3 and 4 show the solid-state structures of **2** and **3**, respectively. We were thus able to ascertain that the overall connectivity of compounds **2** and **3** is identical. The geometry at rhenium is distorted octahedral, with the rhenium centre coordinated by the secondary amine group and the adjacent quinoline nitrogen in a *cis* arrangement. The bromide lies *cis* to both the *N* donors, leading to an overall pseudo-*fac* geometry.

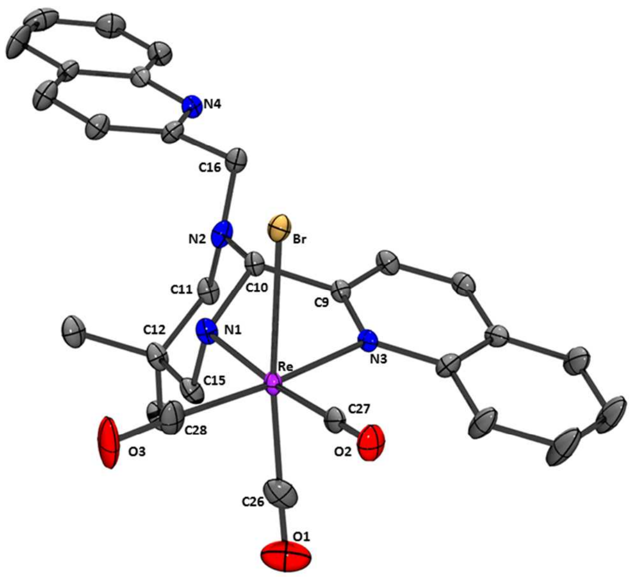

Fig. 3 Molecular structure of **2**. Thermal ellipsoids are shown at the 50% level. Hydrogen atoms are omitted for clarity.

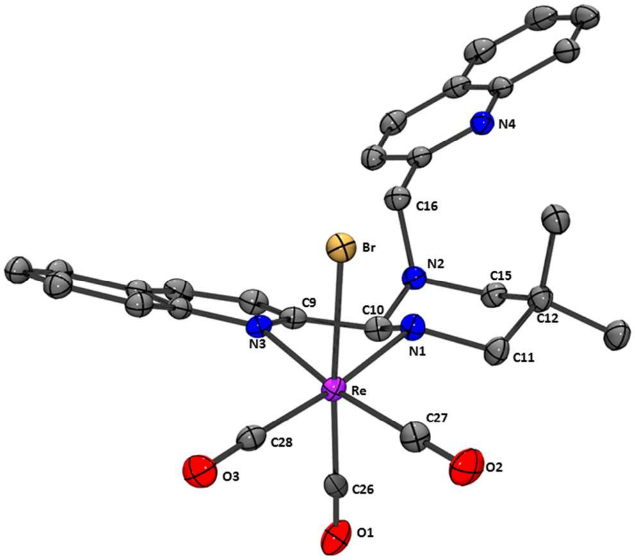

Fig. 4 Molecular structure of **3**. Thermal ellipsoids are shown at the 50% level. Hydrogen atoms are omitted for clarity.

Neither the tertiary amine group, nor the second quinoline species, participate in metal coordination in either complex. Therefore the only difference between **2** and **3** is a ring flip of the pyrimidine, where in **2** the coordinated quinoline lies axially, while in **3** it is equatorial. The uncoordinated quinoline is axial in **3** and disordered between pseudo-axial and pseudo-equatorial in **2**, however as this substituent lies on a tetrahedral nitrogen atom, in solution inversion is expected to equilibrate these conformations.

The highly unsymmetrical nature of both of these species is reflected in the complexity of their respective ^{1}H NMR spectra, with each of the methylene and quinoline hydrogens inequivalent. The fact that these two complexes have a different colour,

Cite this: DOI: 10.1039/c0xx00000x

www.rsc.org/xxxxxx

Table 1 Spectroscopic and Photophysical data for **1** – **3**.

Compound	IR υ(C≡O) ^{a} cm^{-1}	UV-vis λ_{max} ^{b} nm (ε, M^{-1} cm^{-1})	Excitation ^{b} λ_{ex} /nm	Emission ^{b} λ_{em} /nm	Lifetime ^{b} /ns
1	-	273 (12560), 290 (sh, 9560), 296 (sh, 7950), 303 (7680), 310 (sh, 5860), 317 (7950)	350	420	1.3
2	2024 1927 1882	265 (sh, 13,010), 305 (9700), 320 (9060), 349 (sh, 3400), 420 (sh, reaches half height 440)	350	595	250
3	2020 1909 1871	305 (7430), 320 (5160), 335 (3520), 420 (sh, reaches half height 470)	390	595	143

^{a} Neat. ^{b}In CHCl$_3$ solution.

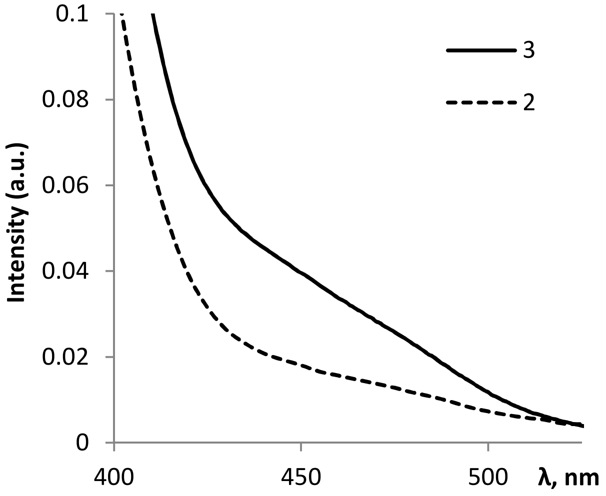

Fig. 5 Section of the UV-vis spectra of **2** and **3**.

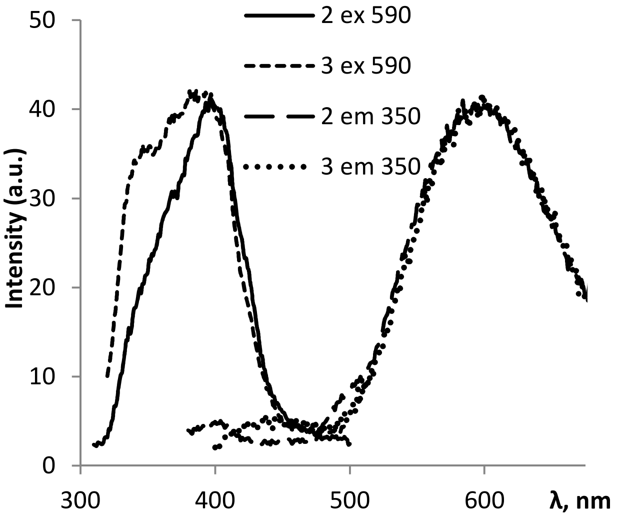

Fig. 6 Emission and Excitation Spectra for **2** and **3**.

regardless of them having identical molecular connectivities, was an entirely unexpected finding and led us to further investigate the optical properties of these species. Photophysical data are summarised in Table 1. The visible difference in appearance between **2** and **3** was reflected in the UV-vis absorption spectrum in which both **2** and **3** have bands centred at ca 350 nm which extend into the visible (*vide infra*), however there are also shoulders apparent on these tails between 420 and 520 nm, which show a large difference in intensity, with **3** having significantly more absorption in the lower energy regions (Fig. 5). These transitions were of great interest as they are broad and featureless, reminiscent of the MLCT bands associated with triplet emission in other rhenium complexes,[11] although these features are rarely associated with complexes in which a single heterocycle coordinates. Indeed, excitation into these absorption bands led to emission in the visible region, with a significant Stokes shift from the excitation maxima (350 nm, **2**, 390 nm, **3)** with both species emitting at 595 nm (Fig. 6). Whilst the excitation spectra were superficially similar, with maxima around 385 and 390 nm, the spectral shapes were clearly different, with a significant shoulder at 350 nm in **2** which is barely visible in **3**, indicating that at least 2 different transitions contribute to both excitation spectra, and that these are of significantly different intensities in the different isomers. The lifetimes of the luminescence, 250 ns (**2**) and 143 ns (**3**), strongly suggest a triplet nature of the excited state, but the significant difference between these values was, again, unexpected for complexes with such similar connectivity.

In order to determine the nature of the electronic transitions involved in the absorption and emission processes, computational studies were undertaken which strongly supported the assignments of the observed shoulders at the UV/vis borderline as MLCT. Time-dependent DFT calculations at the B3LYP/6-31+G(d,p)_SDD level in simulated toluene solvent indicated that the lowest energy absorption bands are dominated by excitation from HOMO to LUMO, and are found at 2.91 eV / 425 nm (**3)** and 2.94 eV / 421 nm (**2**), matching the position of the tails between 420-450 nm in Fig. 5. Inspection of the form of the HOMO and LUMO in each case (Fig. 7) clearly indicate MLCT nature with the HOMOs based mainly on the Re(CO)$_3$Br fragment, and the LUMOs concentrated in the quinoline π system. The most significant difference in orbital plots is that the non-coordinated ring nitrogen N(2) in **2** contributes to the

HOMO, whereas it does not contribute in **3**, indicating a contribution from distant units which appears to be under stereoelectronic control. The classic anomeric model of stereoelectronics in sugars and related systems requires an axial lone pair interacting in an antiperiplanar arrangement with orbitals at the anomeric centre,[12] and it may be significant that such an arrangement is possible in **2**, which has an axially coordinated metal-bound quinoline and an axial N-lone pair (at least in one invertomer) but would be precluded in **3.** An interaction of this sort would involve donation of the N(2) lone pair into the antibonding σ* orbital of the C(10)–C(9) bond. Small differences in the relative bond lengths observed crystallographically are within error (**2**: C(10)–C(9) = 1.530(4) Å; N(2)–C(10) = 1.438(4) Å; **3**: C(10)–C(9) 1.519(4) Å, N(2)–C(10) 1.452(3) Å). However, the involvement of the uncoordinated N(2) lone pair in the electronic transitions is supported by the loss in intensity of the absorption band observed upon protonation (see ESI).† Furthermore, simulated UV-vis spectra from the DFT calculations show that the observed low energy shoulder in **3** matches the calculated transition in which the participation of the non-coordinated ring nitrogen is implicated (see ESI).[13,14]

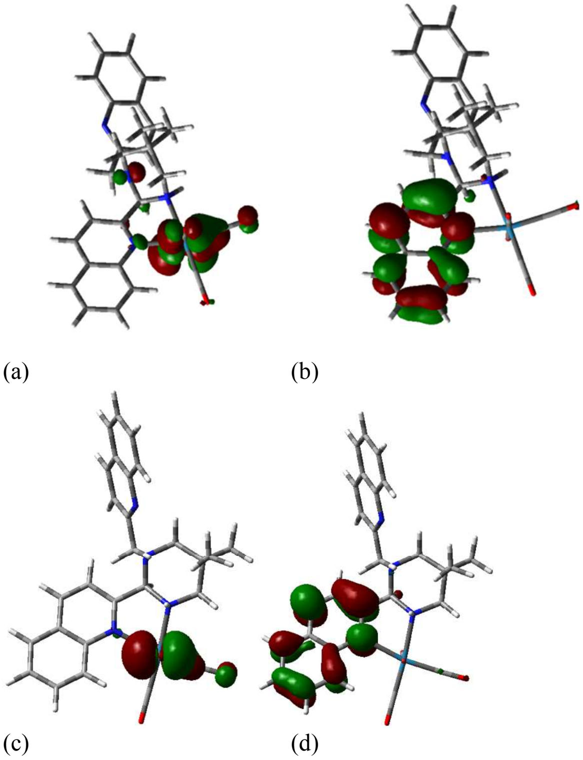
(a) (b)

(c) (d)

Fig. 7 DFT calculated orbital plots for: (a) the HOMO of **2**, (b) LUMO of **2,** (c) HOMO of **3**, (d) LUMO of **3**, plotted at 0.04 au isosurface

Finally, it should be noted that use of the ligands that were initially targeted (of type **A**, Fig. 1) in reactions with Re(CO)$_5$Br give colourless products whereby the quinoline moieties do not participate in coordination and the Re centre is coordinated through the amine nitrogen atoms. In the example that was prepared (compound **4**, ESI)† the resulting complex did not exhibit fluorescence.

Conclusions

A novel pyrimidine ligand incorporating two quinoline substituents has been prepared as a single isomer in a high yielding, one-pot reaction from commercially available starting materials. This ligand forms rhenium complexes selectively as two different isomers, easily separated from each other through precipitation and recrystallization. The complexes have different colours and show different photophysical properties, which we assign as MLCT transitions under stereoelectronic control of a pseudo-anomeric effect. This effect is proposed to be a rare example of stereoelectronic control of photophysical properties, and suggests a possible platform for the design of optical probes for stereochemistry.

We thank the EPSRC UK National Crystallography Service at the University of Southampton for the collection of the crystallographic data and the EPSRC UK National Mass Spectrometry Facility for the collection of mass spectra.

Notes and references

[a] *Department of Chemistry, Lancaster University, Lancaster, LA1 1AE, UK. Tel: +44(0)1524 592557; E-mail: r.platel@lancaster.ac.uk*
[b] *School of Chemistry, Cardiff University, Main Building, Park Place, Cardiff, CF10 3AT, UK.*

† Electronic Supplementary Information (ESI) available: Full experimental, characterization details, ^{1}H and ^{13}C{^{1}H} NMR spectra, crystallographic data for **1-4.** CCDC numbers 1400312-1400315; additional UV-vis spectra for **2** and **3**, details of computational calculations. See DOI: 10.1039/b000000x/

1. D. J. Stufkens and A. Vlcek, Jr, *Coord. Chem. Rev.*, 1998, **177**, 127.
2. M. S. Wrighton and D. L. Morse, *J. Am. Chem. Soc.*, 1974, **96**, 998.
3. M. P. Coogan and V. Fernández-Moreira *Chem. Commun.*, 2014, **50**, 384.
4. S. Ranjan, S.-Y. Lin, K.-C. Hwang, Y. Chi, W.-L. Ching, C.-S. Liu, Y.-T. Tao, C.-H. Chien, S.-M. Peng, and G.-H. Lee, *Inorg. Chem.*, 2003, **42**, 1248.
5. P. Kurz, B. Probst, B. Spingler and R. Alberto, *Eur. J. Inorg. Chem.*, 2006, 2966.
6. F. He, Y. Zhou, S. Liu, L. Tian, H. Xu, H. Zhang, B. Yang, Q. Dong, W. Tian, Y. Ma and J. Shen, *Chem. Commun.*, 2008, 3912.
7. P.D. Beer and E.J. Hayes, *Coord. Chem. Rev.*, 2003, **240**, 167.
8. S. R. Banerjee, J. W. Babich and J. Zubieta, *Chem. Commun.*, 2005, 1784.
9. K. E. Henry, R. G. Balasingham, A. R. Vortherms, J. A. Platts, J. F. Valliant, M. P. Coogan, J. Zubieta and R. P. Doyle, *Chem. Sci.*, 2013, **4**, 2490
10. R. M. Beesley, C. K. Ingold and J. F. Thorpe *J. Chem. Soc., Trans.*, 1915, **107**, 1080.
11. L. Sacksteder, M. Lee, J. N. Demas and B. A. DeGraff *J. Am. Chem. Soc.*, 1993, **115**, 8230.
12. R. U. Lemieux, *Pure Appl. Chem.*, 1971, **25**, 527 and references therein.
13. M. Obata, A. Kitamura, A. Mori, C. Kameyama, J.A. Czaplewska, R. Tanaka, I. Kinoshita, T. Kusumoto, H. Hashimoto, M. Harada, Y. Mikata, T. Funabikig, S. Yano, *Dalton Trans*. 2008, 3292.
14. H.C. Bertrand, S. Clède, R. Guillot, F. Lambert, C. Policar, *Inorg. Chem.* 2014, **53** 6204.